Nonlinear Model Predictive Control for Rough-Terrain Robot Hopping

Martin Rutschmann, Brian Satzinger, Marten Byl and Katie Byl

Abstract— **This paper examines and quantifies the theoretical efficacy of a limited look-ahead strategy for hopping robots on rough terrain. Here, a classic spring-loaded inverted pendulum (SLIP) hopper and an actuated, lossy SLIP (ALSLIP) hopper with a more realistic dynamic model that includes an unsprung mass and a series-elastic actuator are each analyzed under conditions where the desired footholds are predetermined according to a stochastic process. We examine the effect of the length of the horizon on the accuracy of foot placement, and we test the robustness of the approach to model uncertainties. Our simulation results show that a model predictive control (MPC) approach is an effective technique for foothold selection, and that a two-step planning horizon for upcoming terrain is theoretically adequate for practical footstep planning in realistically noisy rough terrain running conditions.**

I. INTRODUCTION

Negotiating rough terrain is an often-stated motivation for using legs in robot locomotion. In particular, legs conceptually provide an advantage over wheeled mobility since they allow a robot to use intermittent footholds. In this context, there are two opposing objectives for legged robots: to achieve desired footholds over time and to remain robust to uncertainties. In practice however, foothold selection tends to be strongly coupled to stabilization in legged robots. For example, an effective way to avoid falling down is often to pick a foothold that best allows one to control angular momentum during the next step. To pick a set of arbitrary footholds on upcoming terrain requires some amount of planning.

At present, the state of the art in legged robotics includes some extraordinary examples of good foothold planning capability and of good robustness to disturbances. Achieving both goals at once in the same robot remains an open challenge, however. Legged robots that are successful at good footstep planning often involve stiff, precise limb actuation along with very good sensory data about upcoming terrain. A bipedal example of this is foothold planning for Honda's ASIMO [1], and planning within a motion capture environment for Boston Dynamic's LittleDog [2] is an example among quadruped robots. Zero-moment point (ZMP) techniques provide an effective and popular means of controlling the center of pressure over time, given preselected set of footsteps. Such ZMP control requires lookahead planning, such as preview control [3].

This work is supported in part by DARPA (Contract W911NF-11-1-0077).

M. Rutschmann is with the Swiss Federal Institute of Technology, Zurich (ETH-Zurich). rutmarti@student.ethz.ch

B. Satzinger, M. Byl and K. Byl are with the Robotics Laboratory, University of California, Santa Barbara, CA 93106, USA {bsatzinger, martenbyl, katiebyl}@gmail.com

There are several legged robots that demonstrate remarkable robustness to perturbations. One example is the quadruped BigDog [4], famously capable of recovering even when kicked. Use of hybrid zero dynamic (HZD) control [5] on MABEL has resulted in excellent robustness to upcoming terrain height variation during blind walking [6]. For robust legged locomotion on an extreme range of rugged terrain, the hexapod RHex [7] excels. In all of these examples, leg compliance plays an important role in robustness, and planning particular footholds remains an important challenge.

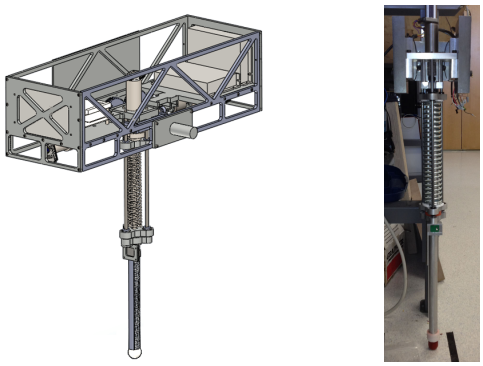

Fig. 1. SLIP-based hopper prototype for boom-mounted testing of MPC foothold planning. Our hopper is the basis for the simulation results throughout. On the right is our most recent prototype which contains design enhancements not discussed in the text.

In past two decades, there has been increasing interest in the use of compliant springs in legged robots [8], [9]. In particular, the Spring Loaded Inverted Pendulum (SLIP) model is an effective model for studying running and hopping motions of both animals (including humans) and robots that has been widely used in the development of legged running robots [10], [11], [12], [13], [14], [15], [16], [17]. For SLIP-based robot models, work has been done to study techniques for adjusting footstep length [18] and to demonstrate robustness to uncertainty [19].

Our work is motivated by the goal of more effectively decoupling the problem of selection of footholds from that of maintaining the overall dynamics of a robot in a reasonable, controllable region of state space. We study a simple but classic spring-based hopper model to represent a running gait, using model predictive control (MPC) to plan motions given a moving, n-step planning horizon of randomly-preselected footholds. A prototype SLIP-based hopper currently under development in our lab is shown in Figure 1. Control of such a system involves selection of a touchdown angle for the leg, to prescribe the overall dynamics of each step, and control of a series-elastic actuator, to moderate the dynamics about this

nominal trajectory. In particular, the actuator allows one both to adjust the overall energy of the system as terrain height varies and to replan future footsteps as new information about terrain is sensed. Given appropriate constraints on the dynamics of the last-planned step, we demonstrate this approach is effective at planning footholds on the fly while remaining both robust to uncertainties in the assumed model parameters. This method is also capable of negotiating rough terrain, to add or remove energy to balance changes in potential energy. "Rough terrain" is loosely defined as a series of target footholds where the vertical height and horizontal distance between footholds changes stochastically from step to step.

The rest of this paper is organized as follows. Section II introduces the classic, energy-conserving SLIP model, and Section III presents a simple but more realistic model (AL-SLIP) that includes both losses due to the unsprung mass and a series elastic actuator that can both replace lost energy and increase controllability of the next apex state. Our Model Predictive Control approach is then described in Section IV. Section V describes the simulation experiments performed and their results, and Section VI provides a conclusion and brief discussion of future work.

II. SLIP MODEL

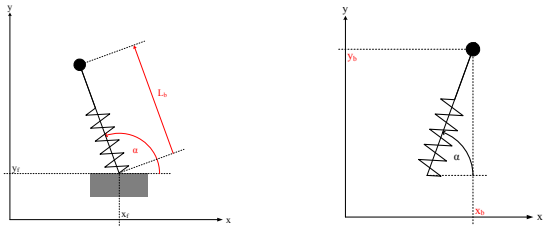

Fig. 2. Definition of coordinates for the Stance Phase (left) and Flight Phase (right).

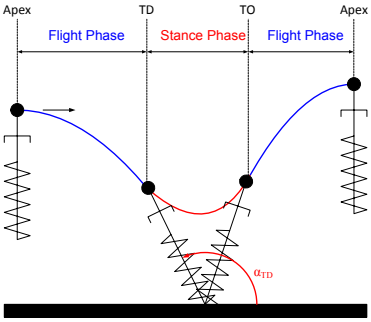

Fig. 3. Illustration of flight and stance phases and take off (TO) and touch down (TD) events

The SLIP model, shown in Figure 2, consists of a point mass m attached to a massless springy leg with a stiffness k. The model dynamics are broken into two phases: 1) flight phase where there is no ground contact and 2) stance phase where the foot is in contact with the ground. This is illustrated in Figure 3. The flight phase dynamics are those of a ballistic point mass, while the stance phase dynamics are derived under the assumption that the foot pin joint constrains axial motion while allowing free rotation.

The SLIP model assumes that the leg angle α can be chosen arbitrarily in flight, with α at touchdown being the sole control variable. There is an apex event during each flight phase, when the vertical velocity becomes zero. The apex state consists of the apex height y_{apex}, the horizontal apex position x_{apex}, and the horizontal apex velocity $\dot{x}_{apex}$

A. Flight Phase Dynamics

As noted earlier the flight phase dynamics are simply those of a point mass following a ballistic trajectory and are expressed as:

$$\ddot{x}_b = 0 \quad (1)$$
$$\ddot{y}_b = -g. \quad (2)$$

B. Stance Phase Dynamics

The stance phase dynamics are expressed as

$$\ddot{L_b} = -\frac{k}{m}(L_b - L_f - L_{k0}) - g\sin(\alpha) + L_b\dot{\alpha}^2 \quad (3)$$
$$\ddot{\alpha} = \frac{-2\dot{L_b}\dot{\alpha} - g\cos(\alpha)}{L_b} \quad (4)$$

where α is the angle between the leg and the ground plane (Figure 2). The nonlinear equations (3) and (4) can not be solved in closed form, and instead are simulated using ode45.

C. Touch-Down and Take-Off Initial Conditions

At touch-down and take-off, we need to transform to and from the Cartesian flight dynamics and polar stance dynamics. During flight, the leg length is always L_0; hence, the initial stance leg length L_b is L_0. The initial touch-down angle α_{TD} is set by the controller during flight. The initial $\dot{\alpha}$ and $\dot{L_b}$ are defined by the velocity of the body at touch-down as

$$\dot{\alpha} = \frac{-\sin(\alpha_{TD})\dot{x_b} + \cos(\alpha_{TD})\dot{y_b}}{L_0} \quad (5)$$
$$\dot{L_b} = \cos(\alpha_{TD})\dot{x_b} + \sin(\alpha_{TD})\dot{y_b}. \quad (6)$$

Take-off occurs when the leg extends to length L_0. At this moment, the position of the body can be calculated as:

$$x_b = x_f + \cos(\alpha)L_0 \quad (7)$$
$$y_b = y_f + \sin(\alpha)L_0 \quad (8)$$

The Cartesian velocities are expressed as:

$$\dot{x_b} = \cos(\alpha)\dot{L_b} - \sin(\alpha)\dot{\alpha}L_0 \quad (9)$$
$$\dot{y_b} = \sin(\alpha)\dot{L_b} + \cos(\alpha)\dot{\alpha}L_0 \quad (10)$$

III. ALSLIP MODEL

The Actuated Lossy SLIP (ALSLIP) model is an extension of the basic SLIP model. It includes an actuator of length L_a in series with the spring and with an unsprung foot mass. Because of the unsprung mass, some energy will be lost at each touchdown event. This energy loss can be compensated for by the series actuator during stance. Figure 4 shows the ALSLIP parameters. Note that the addition of the leg mass and actuator yield modified stance and flight dynamics. Table I gives parameter values used in simulation. These values are chosen to match a prototype robot under development within our lab group.

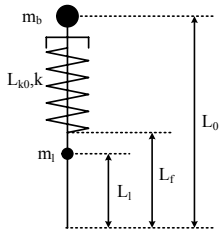

Fig. 4. Illustration of the ALSLIP parameters

Parameter	Description	Value	Unit
m_b	Mass of the body	7	$[kg]$
m_l	Mass of the leg. The leg mass is unsprung and therefore responsible for the losses of the robot	0.7	$[kg]$
L_0	Length of the leg during flight	0.5	m
L_f	Length of fixed part of the leg	0.3	$[m]$
L_l	Distance between the foot and the leg mass.	0.2	$[m]$
L_{k0}	Length of the uncompressed spring. This length should be bigger than or equal to $L_0 - L_f$.	0.2245	$[m]$
k	Spring constant	2800	$[N/m]$
g	Earth gravity	9.81	$[m/s^2]$

TABLE I
PARAMETERS FOR ALSLIP MODEL

A. Flight Dynamics

The flight dynamics for the actuated, lossy model are the same as for the ideal SLIP model, except that the center of mass (COM) will have moved due to presence of the foot mass m_l. It is still assumed that the leg angle can be changed instantaneously during flight.

B. Stance Dynamics

The equations of motion for the stance phase are now

$$\ddot{L_b} = -\frac{k}{m}(L_b - L_a(t) - L_f - L_{k0}) - g\sin(\alpha) + L_b\dot{\alpha}^2 \quad (11)$$

$$\ddot{\alpha} = \frac{-g\cos(\alpha)(L_b m_b + L_l m_l) - 2L_b\dot{L_b}m_b\dot{\alpha}}{L_b^2 m_b + L_l^2 m_l} \quad (12)$$

C. Touch-Down and Take-Off Initial Conditions

Once again, we need to transform between coordinate frames at take-off and touchdown. As for the SLIP model, $L_b = L_0$ at touchdown. We assume that the leg angle is driven to the desired angle during flight. Hence the velocity of the leg mass and the velocity of the body mass are assumed to be equal to the velocity of the center of mass. The initial $\dot{L_b}$ is calculated using (6). To calculate the initial angular velocity, we first need to calculate the angular momentum about the foot:

$$\mathbf{L} = (L_0 m_b + L_l m_l)(-\sin(\alpha_{TD})\dot{x_b} + \cos(\alpha_{TD})\dot{y_b}) \quad (13)$$

The initial angular velocity of the leg can be calculated as:

$$\dot{\alpha} = \frac{\mathbf{L}}{L_0^2 m_b + L_l^2 m_l} \quad (14)$$

At take-off, the Cartesian velocity of the center of mass can be calculated:

$$\dot{x_c} = \frac{\cos(\alpha)\dot{L_b} - \sin(\alpha)\dot{\alpha}(L_b + L_l)}{m_b L_b + m_l L_l} \quad (15)$$

$$\dot{y_c} = \frac{\sin(\alpha)\dot{L_b} + \cos(\alpha)\dot{\alpha}(L_b + L_l)}{m_b L_b + m_l L_l} \quad (16)$$

Complete derivations of the dynamics can be found in [20].

IV. CONTROL DESIGN

Under the assumption that a sequence of foothold locations $r[i]$ have already been determined, it is then our goal to compute a control policy so that the hopper lands on those footholds as closely as possible. We have used finite horizon nonlinear Model Predictive Control (MPC) [21] to accomplish this.

By considering a discrete-time system with each sample $x[k]$ being the apex state, and $u[k]$ being the touchdown angle, the SLIP/ALSLIP models can be analyzed in the form $x[k+1] = f(x[k], u[k])$, where f is a state transition function from apex state to apex state.

In the MPC formulation of the problem, a sequence of future touchdown angles $u[k], ...u[k+N-1]$ are determined in order to minimize a given cost function J:

$$J(\hat{x}[k+1], ..., \hat{x}[k+N], u[k], u[k+1], ..., u[k+N-1]) \quad (17)$$

This minimization is subject to the constraints

$$\hat{x}[j+1] - f(\hat{x}[j], u[j]) = 0, j \in [k+1, ..., N-1] \quad (18)$$

$$\hat{x}[k+1] - f(x[k], u[k]) = 0 \quad (19)$$

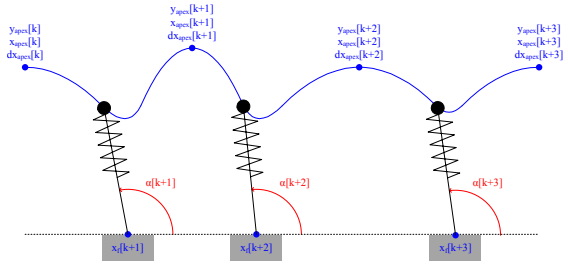

Fig. 5. Illustration of discrete SLIP states and inputs

A. Cost Function

One simple cost function is to sum the squared foothold errors for each step:

$$J = \sum_{i=k+1}^{i=k+N} (r[i] - \hat{x}_f[i])^2. \tag{20}$$

While this works well for minimizing the foot placement error in the short term, simply landing on the next k footholds without considering apex velocity can lead to poor long-term solutions. Although the planned final step may never be carried out because the plan is recomputed after each step, the choice of final step affects the prior apex states. For small values of N this coupling is stronger and can lead to failures.

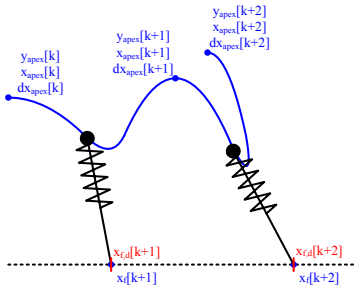

Fig. 6. Example of a solution to the optimization problem in Equation 20 that yields no foothold error and (therefore) no cost but results in poor dynamics at the final planned take-off (horizon=2). Footholds are met exactly, but the final velocity is negative here.

To incorporate a sense of continuity of apex velocity into the cost function, it is modified to reward solutions where the Nth apex velocity is close to the $(N-1)$th apex velocity.

$$J = (\hat{\dot{x}}_{apex}[k+N] - \hat{\dot{x}}_{apex}[k+N-1])^2 + \sum_{i=k+1}^{i=k+N} (r[i] - \hat{x}_f[i])^2. \tag{21}$$

V. SIMULATION EXPERIMENTS

A. SLIP MODEL

In order to verify that minimizing the cost function J (Equation 21) actually leads to a stable control policy, a simulation over 10,000 steps was performed. The commanded footholds were generated by drawing step sizes from a uniform distribution. The maximum step size was chosen to be 0.8 $[m]$, which is less than the maximum possible step size of 0.89 $[m]$. The minimum step size was chosen to be 0.4 $[m]$. All footholds were at the same height. The results of this simulation are shown in the top of Figure 7 for several different horizon sizes.

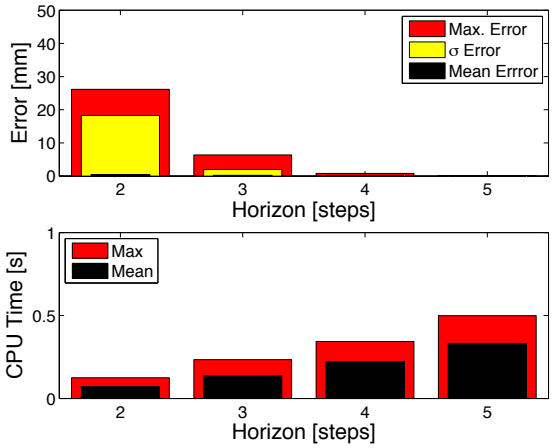

Fig. 7. Foothold Error Statistics for SLIP simulation on flat ground (top). Computation runtime statistics for SLIP accuracy simulation (Bottom).

Increasing the size of the horizon improves both the accuracy and precision of the foothold placement. However, increasing the size of the horizon increases the complexity of the optimization problem to be solved. Since this algorithm will eventually be executed on a robot in real time, a reasonable execution time is required. The bottom plot in Figure 7 shows the mean and maximum computation time for a single step on a typical PC workstation from 2011.

Because the foot size on the hopper robot is on the order of 1 $[cm]$ across, it is not necessary in practice to place the foot with accuracy on a much smaller scale. Furthermore, since a typical flight time is 0.4 $[s]$, a horizon of 3 steps can be chosen so that the next touchdown angle can easily be computed during the flight phase, while still leaving time to move the leg to that position.

B. ALSLIP MODEL

The ALSLIP model is nonconservative, and energy may be added or removed through the actuator. The total energy of the system at the apex consists of kinetic energy due to the horizontal velocity, as well as gravitational potential energy due to the apex height. The "compensated height" z_{apex} is a way of expressing the apex energy in a physically intuitive way by considering the maximum height that could be attained at that energy level.

$$z_{apex} = y_{apex} + \frac{E_{apex,kin}}{gm} = y_{apex} + \frac{\dot{x}_{apex}^2}{2g} \tag{22}$$

The actuator motion is chosen to be a parameterized accelerated single step motion (illustrated and described in

Figure 8). The step delay t_0 was fixed 0.03 seconds, and A was used as as additional control input along with α_{TD}.

The cost function is modified to drive solutions toward a desired compensated height for the next apex, $z_{apex,des}$, with respect to the next foothold location $x_{f,des}[j]$.

$$J = (\hat{\dot{x}}_{apex}[k+N] - \hat{\dot{x}}_{apex}[k+N-1])^2 + \sum_{i=k+1}^{i=k+N} (\hat{x}_f[i] - x_{f,des}[i])^2 + (\hat{z}_{apex}[i] - z_{apex,des})^2 \quad (23)$$

$$z_{apex}[i] = y_{apex}[i] + \frac{\dot{x}_{apex}[i]^2}{2g} - y_{f,des}[i+1], \quad i \in [k+1, ..., k+N-1] \quad (24)$$

$$z_{apex}[k+N] = y_{apex}[k+N] + \frac{\dot{x}_{apex}[k+N]^2}{2g} - y_{f,des}[k+N] \quad (25)$$

$$u[k] = \begin{bmatrix} \alpha[k] \\ A[k] \end{bmatrix} \quad (26)$$

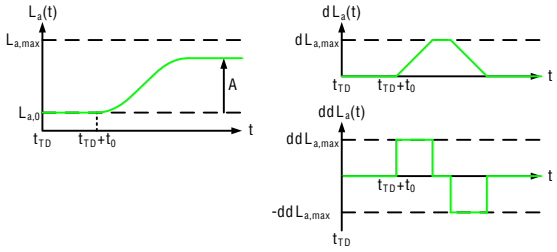

Fig. 8. Parameterized "accelerated step" profile for actuator motion (left). Velocity saturation of the actuator (top right) is set by the voltage limit to the motor (balancing back EMF). The acceleration limit (bottom right) is determined by the peak current (proportional to peak torque).

1) FLAT GROUND: The foot placement experiment previously used with the basic SLIP model is repeated with the ALSLIP formulation. Although the ALSLIP model is compatible with rising and falling terrain, for this experiment the heights are held constant. The horizontal foothold spacings are drawn from a uniform distribution between 0.4 $[m]$ and 0.8 $[m]$. 10,000 steps are performed.

As Figure 9 [top] shows, the ALSLIP foothold placement accuracy is comparable to the SLIP foothold placement accuracy (Figure 7 [top]). Figure 9 [middle] shows that optimizing the touchdown angles $\alpha[k]$ and actuator motions $A[k]$ for the ALSLIP model takes approximately twice as long as optimizing only the touchdown angles $\alpha[k]$ for the SLIP model (Figure 7 [bottom]). Choosing a horizon of 2 steps results in a maximum absolute error of approximately 5 $[cm]$, while a horizon of 3 steps results in a maximum error of approximately 6 $[mm]$, which is reasonably small given a foot size of approximately 1 $[cm]$. However, because these algorithms are intended to be used in real time, it is

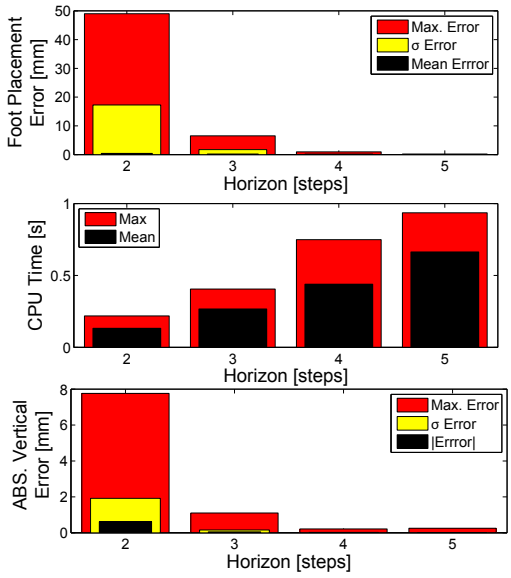

Fig. 9. Foothold Error Statistics for ASLIP simulation on flat ground (top). Computation runtime statistics for ASLIP accuracy simulation (Middle). Compensated height error for ASLIP accuracy simulation (Bottom).

necessary to perform the optimization in as little time as possible. Therefore, for further experiments, a horizon of 2 steps is chosen. Figure 9 [bottom] shows "compensated height" error (Equation 22), which is approximately 1/5th the foot placement error.

2) MODEL MISMATCH: Figures 10.A and 10.D show the effect of a mismatch between the leg mass used in the optimization problem, and the leg mass used in the simulation. The mass mismatch leads to under or overestimation of the predicted apex energy, leading to errors in the compensated height and a bias in foothold placement, due to the change in flight time and stance travel. The same effects are observed for errors in body mass (Figures 10.B and 10.E) and spring stiffness (Figures 10.C and 10.F).

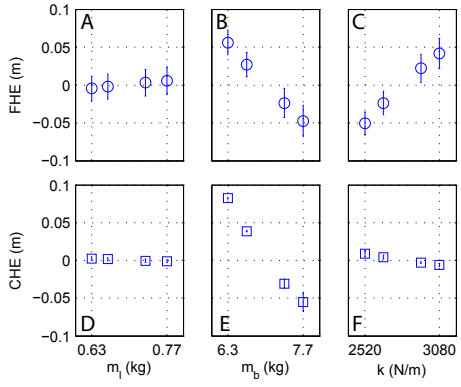

Fig. 10. Foothold Error (FHE) and Compensated Height Error (CHE) under $\pm 10\%$ model variations in m_l, m_b, and k

3) UNEVEN GROUND: To demonstrate the possibility of this controller/robot combination on rough terrain, we tested

the performance of the algorithm on uneven ground. In these tests, the horizontal footholds are drawn from a uniformly distributed random variable between 0.3 [m] and 0.7 [m] while the vertical footholds were drawn independently from a uniform distribution between -0.1 [m] and +0.1 [m]. The results are shown in Figure 11 and are similar to the results on flat ground Figure 9. A video showing an animation of an uneven ground simulation has been submitted with this paper.

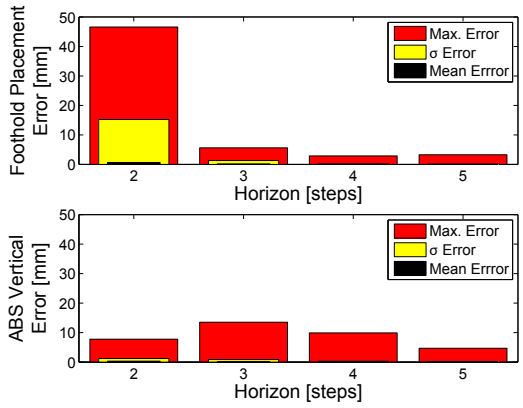

Fig. 11. Foothold Error Statistics for ASLIP simulation on rough ground (top). Compensated height error for ASLIP accuracy simulation on rough ground (bottom).

VI. CONCLUSIONS AND FUTURE WORK

In this paper, we present a novel MPC approach for a hopping robot, designed with a view toward allowing robust foothold planning while minimizing both the computational cost and the look-ahead horizon. We then evaluate its performance in simulations of both ideal and lossy SLIP models with a series elastic actuator to adjust mid-stance dynamics. We demonstrate that this approach should theoretically be effective over both flat and uneven terrain with footstep lengths varying between 80 and 160 percent of leg length, and for the ASLIP hopper step heights of up $\pm 20\%$ of the leg length. To achieve a foot placement accuracy to within one percent of leg length requires a lookahead of three steps for foothold planning. We note that failures (falling down) were never observed during the experiments described in this paper, for example. Also, we note briefly that initial simulations on a more realistic dynamic model that includes a body inertia and both measurement and process noise, rather than an idealized no-noise point mass model, demonstrate that this approach is practical for a more realistic, Raibert-style hopping robot model. As future work, we plan to test this MPC approach experimentally, using a novel hopper prototype currently under development in our group [22], shown in Figure 1. The MPC approach we have described provides a novel methodology to address the important, open challenge of decoupling the problem of foothold selection from that of remaining stable during fast legged locomotion in the presence of moderate noise.

REFERENCES

[1] J. Chestnutt, M. Lau, K. M. Cheung, J. Kuffner, J. K. Hodgins, and T. Kanade, "Footstep planning for the honda asimo humanoid," in *Proceedings of the IEEE International Conference on Robotics and Automation*, April 2005.

[2] K. Byl, A. Shkolnik, S. Prentice, N. Roy, and R. Tedrake, "Reliable dynamic motions for a stiff quadruped," in *Proc. of the 11th Int. Symposium on Experimental Robotics (ISER)*, 2008.

[3] S. Kajita, F. Kanehiro, K. Kaneko, K. Fujiware, K. Harada, K. Yokoi, and H. Hirukawa, "Biped walking pattern generation by using preview control of zero-moment point," in *ICRA IEEE International Conference on Robotics and Automation*, pp. 1620–1626, IEEE, Sep 2003.

[4] R. Playter, M. Buehler, and M. Raibert, "Bigdog," in *Proc. SPIE*, vol. 6230, 2006.

[5] E. R. Westervelt, J. W. Grizzle, C. Chevallereau, J. H. Choi, and B. Morris, *Feedback Control of Dynamic Bipedal Robot Locomotion*. CRC Press, Boca Raton, FL, 2007.

[6] K. Sreenath, H.-W. Park, I. Poulakakis, and J. W. Grizzle, "A compliant hybrid zero dynamics controller for stable, efficient and fast bipedal walking on MABEL," *The International Journal of Robotics Research*, vol. 30, pp. 1170–1193, August 2011.

[7] R. Altendorfer, D. E. Koditschek, and P. Holmes, "Stability analysis of legged locomotion models by symmetry-factored return maps," *International Journal of Robotics Research*, vol. 23, pp. 979–999, Oct-Nov 2004.

[8] R. M. Alexander, "Three uses for springs in legged locomotion," *The International Journal of Robotics Research*, vol. 9, pp. 53–61, April 1990.

[9] G. Pratt, M. Williamson, P. Dillworth, J. Pratt, and A. Wright, "Stiffness isn't everything," in *Proceedings of the 4th International Symposium on Experimental Robotics (ISER)* (O. Khatib and J. Salisbury, eds.), vol. 223, pp. 253–262, Springer Berlin / Heidelberg, 1997.

[10] M.H.Raibert, M. Chepponis, and H. Brown, "Running on four legs as though they were one," *IEEE Journal of Robotics and Automation*, vol. 2, no. 2, pp. 70–82, 1986.

[11] T. A. McMahon and G. C. Cheng, "The mechanics of running: How does stiffness couple with speed?," *Journal of Biomechanics*, vol. 23, no. Supplement 1, pp. 65–78, 1990.

[12] G. Zeglin and B. Brown, "Control of a bow leg hopping robot," in *Proceedings of the 1998 IEEE International Conference on Robotics and Automation*, vol. 1, pp. 793 – 798, IEEE, May 1998.

[13] U. Saranli, W. Schwind, and D. Koditschek, "Toward the control of a multi-jointed, monoped runner," in *Proc. IEEE International Conference on Robotics and Automation (ICRA)*, pp. 2676 – 2682, 1998.

[14] R. M. Ghigliazza, R. Altendorfer, P. Holmes, and D. Koditschek, "A simply stabilized running model," *SIAM Review*, vol. 47, no. 3, pp. 519–549, 2005.

[15] I. Poulakakis and J. Grizzle, "Monopedal running control: Slip embedding and virtual constraint controllers," in *IEEE/RSJ Int. Conf. on Intelligent Robots and Systems (IROS)*, 2007.

[16] A. Sato and M. Buehler, "A planar hopping robot with one actuator: design, simulation, and experimental results," in *Proc. IEEE/RSJ International Conference on Intelligent Robots and Systems (IROS)*, vol. 4, pp. 3540–3545, 2004.

[17] D. Koepl and J. Hurst, "Force control for planar spring-mass running," in *Proc. IEEE Conference on Intelligent Robots and Systems (IROS)*, Sep 2011.

[18] J. Hodgins and M. Raibert, "Adjusting step length for rough terrain locomotion," *IEEE Transactions on Robotics and Automation*, vol. 7, pp. 289–298, June 1991.

[19] K. Harbick and G. S. Sukhatme, "Robustness experiments for a planar hopping control system," *International Conference on Climbing and Walking Robots*, Sep 2002.

[20] M. Rutschmann, "Control of a planar, one legged hopping robot model on rough terrain," Master's thesis, ETH-Zurich, 2012.

[21] R. Findeisen and F. Allgwer, "An introduction to nonlinear model predictive," in *21st Benelux Meeting on Systems and Control, Veidhoven*, pp. 1–23, 2002.

[22] K. Byl, M. Byl, M. Rutschmann, B. Satzinger, L. van Blarigan, G. Piovan, and J. Cortell, "Series-elastic actuation prototype for rough terrain hopping," in *Proc. International Conference on Technologies for Practical Robot Applications(TePRA)*, accepted, 2012.